



# Excited charmonium decays by flux-tube breaking and the $\psi'$ anomaly at CDF

Philip R. Page\*

*Theoretical Physics, University of Oxford, 1 Keble Road, Oxford OX1 3NP, UK*

February 1995

## Abstract

The hadronic decay of radially and orbitally excited charmonium above charm threshold by  $^3P_0$  pair creation and chromoelectric flux-tube breaking is discussed in an harmonic oscillator approximation. We find independent evidence from a study of widths for a 2S admixture in the predominantly 1D state  $\psi(3770)$ , and explore the possibility of metastable radially excited  $2\ ^3P_{0,1,2}$  states being a source of the anomalously large production of  $\psi'$  at the Tevatron. At least one of them is expected to be narrow as a consequence of the existence of nodes in the radial wave function.

---

\*E-mail : p.page@physics.oxford.ac.uk

# 1 Introduction

Recently  $\psi'$  enhancement at CDF [1] has generated considerable interest. This may currently be the largest discrepancy between the predictions of the standard model and experiment, and arises because the behaviour of QCD in the strongly interacting region is inadequately understood theoretically. There are four possible sources of enhanced  $\psi'$  discussed in the literature [2, 3, 4, 5]:  $2^{-+} c\bar{c}$  below the  $D^*D$  threshold [2, 3] ( $D = 0^-$  and  $D^* = 1^-$ ), radial  $\chi$ -states (i.e. 2P charmonia) [3, 4], hybrid charmonium [3] and  $\psi'$  with a  $c\bar{c}gg$ -component [5]. Investigation indicated that  $2^{-+}$  is an unlikely candidate [2, 3] unless  $\psi'$  contains significant  ${}^3D_1$  in its wave function. Detailed study [4] of fusion and fragmentation contributions to the production of radial  $\chi$ -states indicated that they could explain the  $\psi'$  excess if they are very narrow [3, 4] ( $\sim 1$  MeV). We investigate whether this is likely or even possible in a QCD inspired model known to be successful for light hadrons [6], namely the non-relativistic flux-tube model of Isgur and Paton [7], which is related closely to the phenomenologically successful [8]  ${}^3P_0$ -model [9]. The extension of earlier work on light mesons [6] to charmed hadrons is novel in its own right, and will form the basis for a subsequent study [10] of hybrid charmonium.

The strategy is to study first the  $D\bar{D}$  width of  $\psi(3770)$ . This is the cleanest example [11], being a natural 1D-2S candidate. The only real uncertainty is the 1D/2S-mixing, though  $e^+e^-$  and  $\gamma$ -transitions suggest a dominantly 1D state. We find that the width fits with parameters determined elsewhere [6, 12, 13, 14, 15]; and discover that the next potential  $c\bar{c}$  state of higher mass, the 3S [16], would not enable sensible fitting of the  $\psi(3770)$  widths.

It is encouraging that the width of  $\psi(3770)$  fits well in this picture. In fact, it fits in so well that we find the need to constrain the model parameters by also fitting energetically higher lying states, such as  $\psi(4040)$ ,  $\psi(4160)$  and  $\psi(4415)$ , to experiment.

When the model is applied to calculations of the widths of radial  $\chi$ -states the results depend rather critically on the mass of these states, and hence the phase space available for their  $DD$  and  $D^*D$  decays. The  $2^{++}$  decays in D-wave into  $DD, D^*D$ , while  $1^{++} \rightarrow DD^*$  are likely to be near to threshold. As anticipated in ref. [3] we find the  $2^{++}$  generally quite narrow ( $\sim 0.5 - 5$  MeV) in the range of predicted masses. The  $1^{++}$  and  $0^{++}$  widths are very sensitive to the nodes of the radial  $\chi$  wave function. It is possible that they are very narrow ( $\sim 1$  MeV), but this would be a coincidental conspiracy, which nevertheless can be attained near the nodes. We find that for sensible parameter solutions to  $\psi(3770)$ , it is likely that some of the  $(0, 1, 2)^{++}$  widths are considerably reduced, which is sufficient for the enhanced production of  $\psi'$  at CDF.

The basic structure of the paper is as follows.

In §2 we discuss the charmonium system and introduce the flux-tube model and the parameter values used. In §3 we fit the  $\psi(3770)$  to experiment and compare the range of possible mixing angles with those obtained from  $e^+e^-$  annihilation. We are encouraged by the consistency of these results, which prompts us to look at the higher radially excited states in §4, and observe to which degree their experimental signatures can be accounted for. The parameters obtained are used in §5 to look at radial  $\chi$ -states and to examine whether they may be a source of the anomalously large production of  $\psi'$  at CDF. We conclude by outlining the experimental consequences.

## 2 Outline of $c\bar{c}$ phenomenology

Earlier work [11, 15, 17, 18] on the charmonium system [19, 20, 21] is extended by taking into account flux-tube breaking [6, 8, 22]. We perform an *analytical calculation* of radially and orbitally excited charmonium decay amplitudes to  $DD$ ,  $D^*D$ ,  $D^*D^*$ ,  $D_sD_s$ ,  $D_s^*D_s$ ,  $D_s^*D_s^*$  and  $D^{**}D$  ( $D^{**} = (0, 1, 2)^+$ ) in a S.H.O. wave function approximation. This approximation allows comparison with previous work [9, 15, 17, 18] in the  ${}^3P_0$ -model, improves the ability to handle future parameter changes, and is known to be an excellent for charmonia and charmed mesons<sup>1</sup>. The calculation is performed in the approximation where the inverse radii  $\beta$  of the outgoing mesons are identical. The main reason for this simplification is that the  $D^{**}$ ,  $D_s$ ,  $D_s^*$ ,  $D^*$  and  $D$  are expected [6] to have similar  $\beta$ 's, and that the flux-tube and  ${}^3P_0$ -models correspond closely in this case (see the next paragraph). Results do not depend critically on this simplification, making it unnecessary to concern ourselves with small corrections.

The flux-tube model decay amplitude [6] by pair creation differs from the familiar  ${}^3P_0$ -model amplitude, although they coincide in the case when  $\beta$  is a *universal constant* for all outgoing mesons. This is shown in Appendix A, §A.2. In this work, we allow variation of  $\beta$ . Hence the two models are not identical, though their qualitative features are similar [8], allowing comparison with earlier studies [9, 15, 17, 18].

The only free parameter in the model is the overall normalization of decays  $\frac{a\bar{c}}{9\sqrt{3}}\frac{1}{2}A_{00}^0\sqrt{\frac{fb}{\pi}}$  (eqn. 11, Appendix B). This dimensionless factor is common with light meson decays and was phenomenologically found to equal 0.64 [6] for creating light quark pairs with  $u$ ,  $d$  and  $s$  flavours<sup>2</sup>. We adopt it here; thus implying that  $c\bar{c}$  widths are predicted *independently*.

From the ISGW non-relativistic fit [23] to spin-averaged meson masses we take the string tension  $b = 0.18 \text{ GeV}^2$ , and the constituent-quark masses  $m_{u,d} = 0.33 \text{ GeV}$ ,  $m_s = 0.55 \text{ GeV}$  and  $m_c = 1.82 \text{ GeV}$ . Meson masses are taken to be the PDG masses [24], and where not available (which is also the case for  ${}^3P_1/{}^1P_1$  mixing angles) motivated by spectroscopy predictions [16], adjusted in absolute value relative to known masses. The procedure for the calculation of widths is outlined in refs. [6] and [25, §2]<sup>3</sup>.

The experimental total decay widths in MeV are [24] :

$$\begin{aligned}
 \psi(3770) &\rightarrow DD \ddagger & 23.6 \pm 2.7 \\
 \psi(4040) &\rightarrow DD \ddagger, D^*D \ddagger, D^*D^* \ddagger, D_sD_s & 52.0 \pm 10.0 \\
 \psi(4160) &\rightarrow DD, D^*D, D^*D^*, D_sD_s, D_s^*D_s & 78.0 \pm 20.0 \\
 \psi(4415) &\rightarrow DD, D^*D, D^*D^*, D_sD_s, D_s^*D_s, D_s^*D_s^*, D^{**}D & 43 \pm 15
 \end{aligned} \tag{1}$$

where we indicated the dominant<sup>4</sup> decay modes considered in this work, and  $\ddagger$  indicates modes that have been observed [24]. The modes indicated in eqn. 1 are assumed to dominate over decays to  $c\bar{c} + \text{mesons}$ . In the next section we shall calculate these

<sup>1</sup> When expanding full numerical wave functions the overlap with the corresponding radially excited S.H.O. wave function is typically found to be dominant, e.g. 99.8% ( $D, D^*$ ), 97.7% ( $\psi(4040)$ ) and 97.0% ( $\psi(4415)$ ) [15] for appropriately chosen  $\beta$ . The nodal positions in wave functions and decay amplitudes are also well approximated [15].

<sup>2</sup> Suppressions of 1 [17, 18],  $m_u/m_s$  [17] and  $(m_u/m_s)^2$  [11] in amplitude have been employed for  $s\bar{s}$  creation relative to  $u\bar{u}, d\bar{d}$  creation. We adopt the first.

<sup>3</sup>We employ for the masses  $\bar{M}$  [6] the values 1.97 GeV ( $D, D^*$ ), 2.07 GeV ( $D_s, D_s^*$ ), 2.44 GeV ( $D^{**}$ ), 3.76 GeV ( $\psi(3770)$ ), 4.015 GeV ( $\psi(4040)$ ), 4.15 GeV ( $\psi(4160)$ ), 4.39 GeV ( $\psi(4415)$ )

<sup>4</sup> OZI forbidden decays are expected to be small (e.g. experimental indications are that  $\psi(3770) \rightarrow \psi\pi\pi$  has a width of  $\sim 20 - 80 \text{ keV}$  [27]). Also,  $\psi(4415)$  decays to e.g.  $D(2S)D$ ,  $D^{**}D^*$ ,  $D_s^*(2S)D_s^*$  and  $D_s^{**}D_s^*$  are expected [16, 24] to be kinematically forbidden.

Table 1: The outgoing meson on-shell CM momentum  $p_B$  in GeV.

	$p_B$		$p_B$
$\psi(3770) \rightarrow DD$	0.26	$\psi(4415) \rightarrow DD$	1.18
$\psi(4040) \rightarrow DD$	0.77	$\psi(4415) \rightarrow D^*D$	1.06
$\psi(4040) \rightarrow D^*D$	0.57	$\psi(4415) \rightarrow D^*D^*$	0.92
$\psi(4040) \rightarrow D^*D^*$	0.21	$\psi(4415) \rightarrow D_s D_s$	1.00
$\psi(4040) \rightarrow D_s D_s$	0.45	$\psi(4415) \rightarrow D_s^* D_s$	0.84
$\psi(4160) \rightarrow DD$	0.92	$\psi(4415) \rightarrow D_s^* D_s^*$	0.65
$\psi(4160) \rightarrow D^*D$	0.75	$\psi(4415) \rightarrow D_{2^{++}}^{**} D$	0.44
$\psi(4160) \rightarrow D^*D^*$	0.54	$\psi(4415) \rightarrow D_{1^{+L}}^{**} D$	0.52
$\psi(4160) \rightarrow D_s D_s$	0.67	$\psi(4415) \rightarrow D_{1^{+H}}^{**} D$	0.46
$\psi(4160) \rightarrow D_s^* D_s$	0.41		

contributions to the hadronic width in our model, and sum them up in order to fit them to the total experimental widths in eqn. 1.

### 3 Fitting the overall widths to experiment

#### 3.1 $\psi(3770)$

For some time there has been a need to obtain an overall picture of excited charmonium with modern parameters. The process  $\psi(3770) \rightarrow DD$  produces a  $D$ -meson of momentum  $p_B = 0.26$  GeV (see table 1). The decay happens far from where the widths vanish, i.e. from the nodes in the 1D/2S-amplitude, for all phenomenologically relevant  $(\beta_A, \beta)$ . This, the fact there is only one hadronic decay mode, and that the width has been estimated successfully before [11, 26], make it the cleanest charmonium candidate above charm threshold. We shall now proceed to discuss this state in more detail.

The  $J/\psi$  has unambiguously been identified as dominantly 1S, so the  $c\bar{c}$  state  $\psi(3770)$  must be a higher radial or orbital excitation: most probably, on mass alone, a 1D–2S mixture [16]. This can independently and non-trivially be established by considering its width. We find that the  $\psi(3770)$  width is consistent with it being 1D or 2S, i.e. with a 1D–2S mixture. The alternative “gedanken” assumption that  $\psi(3770)$  is a 3S or 4S state leads to a contradiction: this would imply a width to  $DD$  too small to be consistent with experiment (for  $\beta_A, \beta \sim 0.1 - 1$  GeV). Hence we believe that the 1D-2S nature of  $\psi(3770)$  established from width considerations, being consistent with mass spectroscopy, is significant.

Noting that the  $\psi'(3685)$  is predominantly 2S, we expect  $\psi(3770)$  to be mainly 1D, with a 2S admixture<sup>5</sup> as  $|\psi(3770)\rangle = \cos\theta |1D\rangle + \sin\theta |2S\rangle$ . In figure 1 we indicate regions in parameter space where  $\psi(3770)$  can be fitted to experiment as a 1D–2S mixture for various  $\theta$ . The fact that the width can be fitted at all is non-trivial, as will be briefly outlined. If we mix the 1D and 2S decay amplitudes as a new amplitude  $f = \cos\theta 1D + \sin\theta 2S$ ,

<sup>5</sup> We neglect 1S admixture for the following reason : Although our calculation shows that taking  $\psi(3770)$  as pure 1S is sensible for  $\beta_A \sim 0.1 - 0.5$  GeV and  $\beta \sim 0.2 - 0.8$  GeV, and it is known that 1S mixing in  $\psi(3770)$  can be significant [36] for spin-dependent forces; it is small in coupled channel treatments [11, 29, 37]. The latter models successfully reproduce the experimental 2S admixture.

then  $f^2 \leq (1D)^2 + (2S)^2$ ; with the maximum of  $|f|$  occurring at  $\tan\theta = 2S/1D$  and the minimum  $f = 0$  at  $\tan\theta = -1D/2S$ . Clearly there is a large range of widths that the mixed state can have as  $\theta$  is varied. There is still a restriction, though: in regions where  $(1D)^2 + (2S)^2 < 24 \pm 3$  MeV, the  $\psi(3770)$  total width  $f^2 \leq (1D)^2 + (2S)^2$  cannot be fitted for any  $\theta$ . However, there is a large region where  $f$  is large enough to reproduce experiment.

We can restrict the parameter space  $(\beta_A, \beta)$  by incorporating *theoretical prejudice* about the  $\beta$ 's.  $D, D^*$  and  $D^{**}$  have  $\beta$  in the region<sup>6</sup> 0.30 – 0.70 GeV; and  $\psi(2S)$  and  $\psi(1D)$  have  $\beta_A = 0.30 - 0.55$  GeV. From figure 1 we note that  $\psi(3770)$  can be fitted for any  $\theta$  in this region of parameter space, although a *sizable 2S admixture* with  $\sin\theta \sim 30 - 45$  % appears to be preferred. This will be reinforced when we fit more massive states in §3.2.

It can be estimated<sup>7</sup> from the observed  $e^+e^-$ -widths of  $\psi'$  and  $\psi(3770)$  that *either*  $\sin\theta = 17\%$  [27] or  $23\%$  [28] *or*  $\sin\theta = -49\%$  [27] or  $\sin\theta = -44\%$  [28], employing our convention for  $\theta$ . Clearly our analysis prefers  $\sin\theta > 0$ , concurring with findings on the detailed analysis of  $\psi\pi\pi$  [27] and  $c\bar{c}$  radiative [28] decays. This also in agreement with theoretical calculations in the coupled channel formalism, which find  $\sin\theta = 17\%$  [11] or  $20\%$  [29].

Given that the overall normalization of decays was taken from *light meson spectroscopy* as part of a unified study, in contrast to earlier  $c\bar{c}$  calculations [15, 17, 18, 22, 30], we do not regard the disagreement of our estimate with that from  $e^+e^-$ -widths as significant. Our determination of the 2S admixture in  $\psi(3770)$  is hence broadly consistent with its  $e^+e^-$  width and the phenomenology of the  $\psi'$ . We thus consider  $(\beta_A, \beta)$  consistent with a realistic and dominant 1D component in  $\psi(3770)$ , but with a sizable 2S admixture of  $\sim 30\%$  in amplitude.

In summary we conclude that this model of decay by flux-tube breaking can successfully account for the  $\psi(3770)$  as a 1D–2S mixture in this study of widths, consistent with *both* the *a priori* theoretical estimates for  $(\beta_A, \beta)$  and the restrictions on  $\theta$  from  $e^+e^-$ -widths. These conclusions based on its width are also in line with mass spectroscopy. In the next section we shall find that higher states can also be described with varying degrees of success.

## 3.2 Higher mass charmonium

As far as states more massive than  $\psi(3770)$  are concerned, we are led to identify them as 3S–2D mixtures, or higher radial excitations, due to the existence of convincing candidates for 1S, 2S and 1D states. The  $\psi(4160)$  and  $\psi(4040)$  (which may be either simple resonances or a collection of states), should at least contain the 3S and 2D states, otherwise the  $\psi(4415)$  must be 3S or 2D, leading to a contradiction: the 1S, 2S, 3S, 1D and 2D wave functions produce  $\psi(4415)$  total widths too large to be consistent with experiment (for  $\beta_A, \beta \sim 0.2 - 0.8$ ). Hence by default the natural interpretation of  $\psi(4160)$  and  $\psi(4040)$  is that they are 3S–2D mixtures. They can be fitted consistently with experiment in the phenomenologically relevant region  $\beta_A, \beta \sim 0.3 - 0.6$ . Also,  $\psi(4415)$  can be fitted as 4S for  $\beta_A \sim 0.3 - 0.6$  GeV and  $\beta \sim 0.4 - 0.6$  GeV. We shall hence adopt<sup>8</sup> these assignments, which are in agreement with mass spectroscopy [16, 31].

---

<sup>6</sup> It is estimated that  $\beta_{D, D^*} = 0.39$  GeV [23], 0.40 GeV [15], 0.42 GeV [22], 0.49 - 0.55 GeV [13] or 0.54 - 0.66 GeV [6]; and  $\beta_{D^{**}} = 0.34$  GeV [23], 0.42 - 0.49 GeV [13] or 0.45 - 0.54 GeV [6] (on average 0.07 GeV lower than  $\beta_{D, D^*}$ ). For  $c\bar{c}$  the estimates are:  $\beta_{1S} = 0.66$  GeV [23], 0.75 GeV [12] or 0.57 GeV [14];  $\beta_{1P} = 0.50$  GeV [12];  $\beta_{1D} = 0.37$  GeV [14], 0.45 GeV [12] or 0.48 GeV [22].

<sup>7</sup> The experimental uncertainties in  $e^+e^-$ -widths [24] translates into  $\sim 4\%$  uncertainty in  $\sin\theta$ .

<sup>8</sup> We assume no mixing for higher charmonium states for simplicity: it is generally considered to be small [11], e.g.  $\sim 10\%$  [29] in coupled channel models.

Table 2: A selection of widths in MeV *fitting experiment* (see §3). We assume a common  $\beta$  (in GeV) in order to reduce parameters. We allow  $\psi(3770)$  to have  $\beta_A^{\psi(3770)} = \beta_A + 0.1$  GeV (see §3.2), and a 1D-2S mixing angle  $\theta$ , in the decay  $\psi(3770) \rightarrow DD$ . We indicate  $\psi(4160)$  as either 3S or 2D, and the widths of the various decay modes  $\psi(4160) \rightarrow DD, D^*D, D^*D^*$  (P- and F-wave),  $D_sD_s, D_s^*D_s$ .

$\beta_A$	$\beta$	$\psi(3770)$		$\psi(4160)$							
		$\sin \theta$	Total		$DD$	$D^*D$	P	F	$D_sD_s$	$D_s^*D_s$	Total
0.50	0.54	0.3	23	2D	32	1	6	20	4	11	74
0.50	0.54	0.3	23	3S	13	4	34	0	1	20	72
0.42	0.52	0.4	24	3S	17	44	3	0	1	2	67
0.30	0.39	0.5	21	3S	1	22	52	0	5	1	81

Table 3: As in table 2 but for  $\psi(4415)$  decaying to  $DD, D^*D, D^*D^*$  (P-wave),  $D_sD_s, D_s^*D_s, D_s^*D_s^*$  (P-wave),  $D_{2^{**}}, D_{1^{**}L}$  (S- and D-wave),  $D_{1^{**}H}$  (S- and D-wave). Here  $L, H$  indicates the low and high  $J^P = 1^+$  mass states respectively, with a  $^3P_1/{}^1P_1$ -mixing angle of  $\tilde{\theta} = -41^\circ$  [16] (see eqn. 13, Appendix B). We take the  $D_{1^{**}H}$  mass to be 2.45 GeV.

$\beta_A$	$\beta$	$DD$	$D^*D$	$D^*D^*$	$D_sD_s$	$D_s^*D_s$	$D_s^*D_s^*$	$D_{2^{**}}$	$D_{1^{**}L}$		$D_{1^{**}H}$		Total
									S	D	S	D	
0.50	0.54	1	3	1	1	2	0	14	0	17	1	1	41
0.42	0.52	8	22	11	1	0	0	1	0	1	1	0	45

We expect the  $\psi(4160)$  to be the easiest to describe. This is because there is an experimental constraint on the width ratios of  $\psi(4040)$  [17] (see below), casting doubt on whether it is conventional  $c\bar{c}$ . Also, the  $\psi(4415)$  has numerous decays modes (including decays to  $D^{**}D$ ), making its narrowness [17] potentially difficult to understand.

It is theoretically expected that the magnitudes of  $\beta_A$  for higher excited states are smaller than those of lower states (e.g.  $\psi(3770)$  in this case) by  $\lesssim 0.1$  GeV [6]. Allowing for this, we find<sup>9</sup> that all three of the higher states can be accommodated with a 2S admixture in  $\psi(3770)$  of  $\sim 30 - 45$  % in amplitude. It can be seen by comparing figures 1 and 2.

If we choose parameters consistent with a sizable 2S component in  $\psi(3770)$ , figure 2 indicates that it is possible to fit  $\psi(4160)$  as 3S, and to a lesser extent as 2D, in a wide range of theoretically acceptable  $(\beta_A, \beta)$ . If we require  $\beta$  near to the ISGW value [23],  $(\beta_A, \beta) = (0.30, 0.39)$  GeV gives a good fit for most states. Some of these values also allow fits of  $\psi(4415)$  (see tables 2 and 3), e.g.  $(\beta_A, \beta) = (0.42, 0.52)$  GeV, where we find excellent agreement. The point  $(\beta_A, \beta) = (0.50, 0.54)$  GeV, which fits  $\psi(4040)$  in addition (see below), also lies in this region.

We now proceed to discuss the  $\psi(4040)$ . The issue of whether it can be understood as ordinary charmonium has historically been controversial, due to its anomalously large  $D^*D^*$  branching ratio. The large experimental ratios [24]  $R_1 \equiv \Gamma(D^*D) / \Gamma(DD) = 5 - 20$  and  $R_2 \equiv \Gamma(D^*D^*) / \Gamma(D^*D) = 1 - 2.5$  can conceivably be explained by looking for nodes (zero's) [11] in the decay amplitudes corresponding to decays into  $DD$  and  $D^*D$ . This can arise if the kinematics of the decay are controlled by nodes arising from the

<sup>9</sup> This result holds for  $\psi(4040)$  as 3S, and to a lesser extent as 2D; for  $\psi(4160)$  as 3S, and to a lesser extent as 2D; and for a 4S  $\psi(4415)$ .

Table 4: Total widths in MeV at specific  $(\beta_A, \beta)$  (in GeV) *providing an excellent fit to  $\psi(4040)$*  (see §3.2).  $\psi(3770)$  is fitted with a 1D-2S mixing angle  $\theta$  assuming  $\beta_A^{\psi(3770)} = \beta_A + 0.1$  GeV. The  $\psi(4040)$  width ratios  $R_{1,2}$  defined in §3.2 are indicated along with the widths of the various decay modes.  $\psi(4040)$  is constrained to be 3S, implying that  $\psi(4160)$  should be 2D. All decays are in P-wave.

$\beta_A$	$\beta$	$\psi(4040)$							$\psi(3770)$		$\psi(4160)$
		$DD$	$D^*D$	$D^*D^*$	$D_sD_s$	Total	$R_1$	$R_2$	$\sin \theta$	Total	Total
0.50	0.54	2	15	23	5	45	9	1.5	0.3	23	74
0.24	0.23	4	26	34	2	66	6	1.3	0.1	22	41
0.50	0.20	1	14	29	8	52	15	2.0			

radial wave functions of the 3S or 2D states. There is thus the possibility of the  $DD$  and  $D^*D$  amplitudes being near enough to two<sup>10</sup> different nodes or to the same node [17]. We proceed to seek cases  $(\beta_A, \beta)$  where  $R_1$  and  $R_2$  are consistent with experiment. Although  $R_{1,2}$  can be fitted for  $\psi(4040)$  as 2D with  $(\beta_A, \beta) \sim (0.3, 0.2)$ , the total width is too small, leading us to the conclusion that a consistent picture of  $\psi(4040)$  can *only* be obtained with it as 3S. Our search provides three areas in parameter space where the  $\psi(4040)$  may be realized as 3S (see table 4 and figure 2). If in addition we require the  $\psi(3770)$  and  $\psi(4160)$  to be consistent with experiment,  $\psi(4160)$  to be 2D (as a consequence of  $\psi(4040)$  being 3S), and the parameters to be consistent with theoretical estimates, we are restricted to  $(\beta_A, \beta)$  around (0.50,0.54) GeV. This region represents the only area where we can fit *all* experimental data on excited charmonium decays, including the  $\psi(4160)$  and  $\psi(4415)$ , with the  $\psi(3770)$  a 1D-2S mixture as usual (see tables 3 and 4). The region also appears to be related to the one found by Le Yaouanc *et al.* [17], who also identified<sup>11</sup>  $\psi(4040)$  as 3S. This implies that it is possible to fit  $\psi(4040)$  consistent with experiment without contradicting the phenomenology of the other  $\psi$ -states, although it *severely* constrains the parameters, requiring considerable coincidence of parameters [18] and fine tuning of  $\beta_A$  to  $\sim 1 - 3$  %, in order to obtain the correct branching ratios.

The fits obtained for  $(\beta_A, \beta) = (0.42, 0.52)$  and  $(0.50, 0.54)$  GeV above are remarkable in the sense that we can accurately fit *three* amplitudes (i.e.  $\psi(3770)$ ,  $\psi(4160)$  and  $\psi(4415)$ ) to experiment with *two* parameters  $\beta_A$  and  $\beta$ , with the *additional* conclusion that  $\psi(4040)$  can possibly be fitted, and furthermore that the assigned nS, nD classifications are consistent with mass spectroscopy.

In summary we conclude that the higher states may also be accommodated in this model. We have thus established another rung on the  $c\bar{c}$  ladder, highlighting the difficulties associated with  $\psi(4040)$  and  $\psi(4415)$ .

<sup>10</sup> We showed that there exists no  $(\beta_A, \beta)$  for which for which the momenta  $p_B = 0.77$  GeV ( $DD$ ) and  $p_B = 0.57$  GeV ( $D^*D$ ) lie near different nodes in the decay amplitude.

<sup>11</sup> They obtained  $\beta_A = \beta = 0.44$  GeV, but with old parameter values and a mass formula neglecting the difference between  $m_c$  and  $m_u$ .



## 4 $2P$ charmonia and the $\psi'$ anomaly at CDF

The experimental production rate of  $\psi'$  is 30 times larger than theoretical estimates [1] at large transverse momentum in  $p\bar{p}$  collisions at the Tevatron. One proposed source [3, 4] is the production of  $2P$  charmonia followed by their radiative decay  $2^{2S+1}P_J \rightarrow 2^3S_1 + \gamma$ , enhancing the  $\psi'$  rate. This can only happen if the  $2P$  charmonia have small hadronic widths. These states are expected [16, 31] to lie above the  $DD$ -threshold (3.73 GeV), probably above the  $D^*D$ -threshold (3.87 GeV), and possibly above the  $D_sD_s$ -threshold (3.94 GeV) but beneath the  $D^*D^*$ -threshold (4.02 GeV). In these circumstances we find that their hadronic widths may be small.

If the  $2P$  states lie *below* the  $D^*D$ -threshold (say at 3.85 GeV), then the  $2^3P_2$  and  $2^{3,1}P_1$  are narrow :  $2^3P_2$  (because of D-wave phase space) has width 0-4 MeV, and  $2^{3,1}P_1$  is narrow because only decays to  $D^*D$  are allowed.

If the  $2P$  states lie *above* the  $D^*D$ -threshold the  $2^3P_2$  has the unique property that the total width remains small (because of D-wave phase space) at 0 - 7 MeV (3.90 GeV) and 1 - 14 MeV (3.95 GeV). Figure 3 indicates that in the theoretically reasonable region where  $(\beta_A, \beta) \sim (0.3, 0.4) - (0.4, 0.6)$  GeV these widths can be  $\lesssim 1$  MeV if  $(\beta_A, \beta)$  is tuned to only  $\sim (15, 20)$  %. This is of special interest for the resolution of the CDF anomaly. The  $2^{3,1}P_1$  and  $2^3P_0$  states only have small widths if the kinematics of the decay cause the amplitude to be controlled by the nodes arising from the radial wave functions of the  $2P$  states (otherwise the amplitude can be substantial, even near thresholds).

- For decays of  $2^{3,1}P_1$  the S-wave nodes occur in a line of parameter space  $(\beta_A, \beta) \sim (0.3, 0.4) - (0.45, 0.6)$  GeV coinciding with narrow  $2^3P_2$  (see figure 3). It is fascinating that this region coincides with D-wave nodes, reinforcing the narrowness of  $2^{3,1}P_1$ .
- For decays of  $2^3P_0$  the S-wave nodal line occurs for  $(\beta_A, \beta) \sim (0.4, 0.3) - (0.5, 0.6)$  GeV (see figure 3). Estimates [16] suggest this to be the lightest  $2P$  state, and hence possibly narrow (i.e. below the  $D_sD_s$ -threshold, which ensures that  $2^3P_0 \rightarrow D_sD_s$  does not overshadow the decay).

Hence we expect *at least one* of  $2^3P_2$ ,  $2^3P_1$  or  $2^3P_0$  to be narrow; the  $2^3P_2$  being most likely, since obtaining  $2^3P_0$  and  $2^3P_1$  widths of  $\leq 1$  MeV requires fine tuning  $(\beta_A, \beta)$  respectively to  $\sim (4, 7)$  % and  $\sim (1, 1)$  % in figure 3. Theoretically we expect  $\beta_{2P} \sim 0.3 - 0.45$  GeV, tantalizingly in accord with the values where we expect nodes to occur.

Both the best regions in §3 fitting experiment (i.e. near  $(\beta_A, \beta) = (0.42, 0.52)$  and  $(0.50, 0.54)$  GeV) can be consistent with one of the  $2P$  states being very narrow ( $\sim 1$  MeV), depending sensitively on their masses.

If an amplitude lies near a node, it becomes especially sensitive to differential amounts of phase space e.g. for  $D^0\bar{D}^0$  and  $D^+\bar{D}^-$  final states. This sensitivity may be decreased if other small decay modes far from a node swamp the decay. Since  $\delta p_B \sim 1/p_B$ , the change in available phase space is largest when the decay is nearest to threshold, so that amplitude variations<sup>12</sup> are pronounced near thresholds. Hence, when  $2P$  masses are known experimentally, these effects should be incorporated near the various thresholds if there is nodal suppression of an amplitude.

---

<sup>12</sup>We have not considered these effects in §3.1. They are expected to be largest for  $\psi(3770) \rightarrow DD$ , because it is near threshold (see table 1), and the dominant hadronic decay mode. However for realistic  $(\beta_A, \beta)$  it is far from a node, with typically 5 - 15 % variation in width due to varying the phase space of decays to  $D^0\bar{D}^0$  and  $D^+\bar{D}^-$ . So the effect is small compared to variations in  $(\beta_A, \beta)$ .

## 5 Conclusions

Our results from hadronic decays of charmonium are as follows :

- $\psi(3770) \rightarrow DD$  can be understood with the  $\psi(3770)$  as a mixture of  $2^3S_1$  and  $1^3D_1$ . We find that the width fits with parameters determined elsewhere [6, 12, 13, 14]; and discover that the next state of higher mass, the 3S [16], would not enable sensible fitting. We favour a sizable 2S admixture in  $\psi(3770)$  ( $\sim 30\%$  in amplitude), consistent with  $e^+e^-$ -annihilation. This is also in observational agreement with higher states.
- We find further encouragement that the widths of  $\psi(4160)$  and  $\psi(4040)$  fit well if they are 3S–2D mixtures. We note that they do not admit solutions as 2S-1D states.
- $\psi(4160) \rightarrow DD, D^*D, D^*D^*, D_sD_s, D_s^*D_s$  can be understood with the  $\psi(4160)$  as either  $3^3S_1$  or  $2^3D_1$ , depending on the preferred value of  $(\beta_A, \beta)$  in §3. Study of the branching ratios of this state at a  $\tau$ -charm factory could be a rather critical test of its wave function composition.
- $\psi(4040)$  cannot be understood as  $2^3D_1$ , due to an inability to reproduce simultaneously the total width and correct branching ratios into  $DD, D^*D, D^*D^*$ . These are experimentally (neglecting statistical uncertainties) 1 : 8 : 14. Remarkably, the state can be understood as  $3^3S_1$  in three regions of parameter space (see table 4). This, however, severely constrains parameters. Previous interpretations of  $\psi(4040)$  as  $c\bar{c}$  [15] may hence now be invalid due to a change in preferred parameters. This leaves open the possibility of  $\psi(4040)$  being a  $D^*D^*$  molecule [19] or a threshold effect [32] (the state is 10 - 30 MeV above the  $D^*D^*$  threshold with a width of 40 - 60 MeV, and can hence not be treated well in the narrow resonance approximation). There may be several  $1^{--}$  states in the 4.0 - 4.3 GeV region, due to the possible additional existence of a hybrid meson of mass  $\sim 4.2$  GeV [31, 33], but whose  $e^+e^-$  production is suppressed due to the radial wave function vanishing at the origin [31].
- The  $\psi(4415)$  is pinned down to having a 4S wave function. Its total width tends to be small enough only in restricted regions, suggesting that the narrowness [17] of  $\psi(4415)$  remains an interesting issue<sup>13</sup>. It is not easy [30] to identify dominant *decay modes* without fixing  $(\beta_A, \beta)$  and the degree of mixing, as was effectively done in the literature [17, 18, 15], in contrast to earlier expectations [17, 18] where  $D_{2^{*+}}^*D$  was indicated as possibly significant.

Where energetically allowed, decays to  $D_s, D_s^*$  are suppressed by a flavour factor of two, relative to decays to  $D, D^*$ . This, together with P-wave phase space, conspires to make the branching ratios of  $\psi(4040), \psi(4160)$  and  $\psi(4415)$  to  $D$  and  $D^*$  consistently larger than those to  $D_s$  and  $D_s^*$ . This is violated for  $\psi(4040) \rightarrow D_sD_s$ , where the lack of a corresponding experimental width estimate may indicate additional suppression of  $s\bar{s}$  creation [11, 17] (see table 4 and footnote 2).

Radial  $\chi$ -states may be the source of a significant  $\psi'$  cross-section at the Tevatron if their widths are narrow. Their widths depend rather critically on their masses, and hence

---

<sup>13</sup> The narrowness can be increased by increasing the radial excitation. Studies of the  $\psi(4415)$  width [17, 18, 22] and mass [29] tend to find a 4S assignment. A 5S assignment (with an accompanying 4S  $\psi(4160)$ ) has, however, been suggested [28, 30]. This possibility is found to be consistent with experimental widths by our study, and can as such not be ruled out.

the phase space available for their  $DD$  and  $D^*D$  decays. The  $2^{++}$  decays in D-wave into  $DD, D^*D$ , while  $1^{++}$  decays to  $DD^*$  are likely to be near to threshold. As anticipated in ref. [3] we find the  $2^{++}$  generally quite narrow ( $\sim 0.5 - 5$  MeV) in the range of predicted masses, with the narrower widths corresponding to D-wave nodal suppression. The  $1^{++}$  and  $0^{++}$  widths are very sensitive to the nodes of the radial  $\chi$  wave function. It is possible that they are very narrow ( $\sim 1$  MeV), but this would be a coincidental conspiracy. For  $0^{++}$  below the  $D_s D_s$ -threshold, nodal suppression is quite consistent with  $\psi(3770)$  decays. We thus find that for sensible parameter solutions to  $\psi(3770)$ , it is likely that some of the  $(0, 1, 2)^{++}$  widths are considerably reduced. This would suggest placing emphasis on searching for the  $2^3P_2$  in events containing  $\psi'$ . We predict that if its hadronic width is found to be  $\sim 1$  MeV, then the  $2^{3,1}P_1$  may also be found to narrow (depending sensitively on their mass).

The overall consistency of excited charmonium with observation vindicates the expectation that the pair creation amplitude is similar for charmonium and light meson decays (in each case light quarks are created). In view of the slightly exaggerated 2S admixture we obtain in  $\psi(3770)$ , this amplitude may have to be adjusted slightly. This procedure would however not affect the nodes in the  $\chi$  decay amplitude, leaving the  $(\beta_A, \beta)$  where  $\chi$ -states are narrow unaltered.

We highlight the need for improved data on excited charmonia : to confirm whether they are true resonances, to study their branching ratios into various channels and to discover whether some may be narrow. Rather clear signals, in particular in  $e^+e^-$ -annihilation, may also reveal hybrids and molecules.

## Acknowledgements

Thanks to J.M. Richard, K. Lane, S.F. Tuan and A. Wambach for helpful criticism. Special thanks goes to F.E. Close for discussions, motivation and comments. This work was supported in part by the Universities of Cape Town and Oxford.

## A Appendix : The coincidence of flux-tube and $^3P_0$ -model decay amplitudes in limiting cases

For meson decays to mesons the  $^3P_0$  and the flux-tube models coincide in the limit of an infinitely thick flux-tube, i.e. where the pair creation amplitude is constant all over space. This is indicated explicitly in §A.1. It is possible to make a stronger statement : *The  $^3P_0$  and flux-tube models coincide when  $\beta$  is a universal constant for all outgoing mesons, even if the flux-tube has finite thickness.* This is demonstrated in §A.2.

We focus on two initial quarks of mass  $M$ , with pair creation of quarks of mass  $m$ . The decay amplitude of an initial meson A into final mesons B and C can be shown [25, Appendix A] in the rest frame of A (where  $\mathbf{p}_A = 0$ ) to be given by

$$\begin{aligned}
& -\frac{a\tilde{c}}{9\sqrt{3}}(2\pi)^3\delta^3(\mathbf{p}_B + \mathbf{p}_C)\frac{i}{2}Tr(A^T BC)_{flavour}Tr(A^T B\boldsymbol{\sigma}^T C)_{spin} \\
& \quad \times \int d^3\mathbf{r}_A d^3\mathbf{y} \psi_A(\mathbf{r}_A) \exp(i\frac{M}{m+M}\mathbf{p}_B \cdot \mathbf{r}_A)\gamma(\mathbf{r}_A, \mathbf{y}_\perp) \\
& \quad \times (i\nabla_{\mathbf{r}_B} + i\nabla_{\mathbf{r}_C} + \frac{2m}{m+M}\mathbf{p}_B)\psi_B^*(\mathbf{r}_B)\psi_C^*(\mathbf{r}_C) + (B \leftrightarrow C)
\end{aligned} \tag{2}$$

Here ( $B \leftrightarrow C$ ) indicates a term obtained by interchanging the flavour and spin matrices  $B \leftrightarrow C$  and momenta  $\mathbf{p}_B \leftrightarrow \mathbf{p}_C$  in the first term in eqn. 2. For  $c\bar{c}$  decaying by the creation of a  $u\bar{u}$ ,  $d\bar{d}$  or  $s\bar{s}$  pair, only one of the terms contribute (due to  $Tr(A^T BC)_{flavour}$ ); and the space part of the term differs by a sign from the space part of the displayed term in eqn. 2. So from now on it is sufficient just to consider the the displayed term.

The pair creation position  $\mathbf{y}$  [6] is measured relative to the CM of the initial quarks, and  $\mathbf{y}_\perp \equiv -(\mathbf{y} \times \hat{\mathbf{r}}_A) \times \hat{\mathbf{r}}_A$  is a perpendicular ‘‘component’’ of  $\mathbf{y}$  to the initial  $Q\bar{Q}$ -axis  $\mathbf{r}_A$ . The  $Q\bar{q}$ -axes of the final states B and C are  $\mathbf{r}_B = \mathbf{r}_A/2 + \mathbf{y}$  and  $\mathbf{r}_C = \mathbf{r}_A/2 - \mathbf{y}$  respectively [6].

## A.1 Spatially constant pair creation

The pair creation amplitude (or *flux-tube overlap*) is

$$\gamma(\mathbf{r}_A, \mathbf{y}_\perp) = A_{00}^0 \sqrt{\frac{fb}{\pi}} \exp\left(-\frac{fb}{2} \mathbf{y}_\perp^2\right) \quad (3)$$

The thickness of the flux-tube is related inversely to  $f$ . A detailed discussion of these quantities and the structure of eqn. 3 may be found in ref. [6, eqn. A21] and ref. [34]. The estimated values  $f = 1.1$  and  $A_{00}^0 = 1.0$  [25, 34] are used in this work. The infinitely thick flux-tube with  $f = 0$  corresponds to the  ${}^3P_0$ -model [17]. In this case  $\gamma(\mathbf{r}_A, \mathbf{y}_\perp)$  is a constant (which should be normalized to be non-zero), and the  $q\bar{q}$ -pair is created with uniform amplitude anywhere in space. Fourier transforming (a relevant part of) eqn. 2 yields

$$\begin{aligned} & \frac{-i}{2} (2\pi)^3 \delta^3(\mathbf{p}_B + \mathbf{p}_C) \mathbf{e}_\sigma \cdot \int d^3\mathbf{r}_A d^3\mathbf{y} \psi_A(\mathbf{r}_A) \exp\left(i\frac{M}{m+M} \mathbf{p}_B \cdot \mathbf{r}_A\right) \\ & \quad \times \left(i\nabla_{\mathbf{r}_B} + i\nabla_{\mathbf{r}_C} + \frac{2m}{m+M} \mathbf{p}_B\right) \psi_B^*(\mathbf{r}_B) \psi_C^*(\mathbf{r}_C) = \\ & -i\delta^3(\mathbf{p}_B + \mathbf{p}_C) \mathbf{e}_\sigma \cdot \int d^3\mathbf{k}_A (\mathbf{k}_A + \mathbf{p}_B) \psi_A(\mathbf{k}_A) \psi_B^*\left(\mathbf{k}_A + \frac{M}{m+M} \mathbf{p}_B\right) \psi_C^*\left(\mathbf{k}_A + \frac{M}{m+M} \mathbf{p}_B\right) \end{aligned} \quad (4)$$

where we defined  $\psi_{A,B,C}(\mathbf{r}) = (2\pi)^{-3} \int d^3\mathbf{k} \exp(i\mathbf{k} \cdot \mathbf{r}) \psi_{A,B,C}(\mathbf{k})$ .

Taking the  ${}^3P_0$ -model amplitude [35, p. 120], with the  $q\bar{q}$ -pair created with equal but opposite momenta

$$\begin{aligned} & \frac{-i}{2} \sqrt{\frac{4\pi}{3}} \int d^3\mathbf{k}_1 d^3\mathbf{k}_2 d^3\mathbf{k}_3 d^3\mathbf{k}_4 \delta^3(\mathbf{k}_1 + \mathbf{k}_2 - \mathbf{p}_A) \delta^3(\mathbf{k}_1 + \mathbf{k}_3 - \mathbf{p}_B) \delta^3(\mathbf{k}_2 + \mathbf{k}_4 - \mathbf{p}_C) \delta^3(\mathbf{k}_3 + \mathbf{k}_4) \\ & \quad \times Y_{1\sigma}(\mathbf{k}_3 - \mathbf{k}_4) \psi_A\left(\frac{\mathbf{k}_2 - \mathbf{k}_1}{2}\right) \psi_B^*\left(\frac{M\mathbf{k}_3 - m\mathbf{k}_1}{m+M}\right) \psi_C^*\left(\frac{m\mathbf{k}_2 - M\mathbf{k}_4}{m+M}\right) \end{aligned} \quad (5)$$

we can see that it equals the last line of eqn. 4 [15] (with  $\mathbf{p}_A = 0$ ) when we make a change of variables to  $\mathbf{k}_A = (\mathbf{k}_1 - \mathbf{k}_2)/2$  and  $\mathbf{k}_{CM} = \mathbf{k}_1 + \mathbf{k}_2$ . Here  $kY_{1\sigma}(\mathbf{k}) = \sqrt{\frac{3}{4\pi}} \mathbf{e}_\sigma \cdot \mathbf{k}$  was used. We have thus connected the flux-tube and  ${}^3P_0$ -model notation explicitly; showing that *the two models coincide for an infinitely thick flux-tube*; and verifying the expectation that *a zero momentum  $q\bar{q}$ -pair corresponds to complete freedom in creating the pair anywhere in space*.

## A.2 Outgoing mesons of equal “size”

The incoming and outgoing mesons have S.H.O. wave functions with inverse radii  $\beta_A$  and  $\beta$  respectively. We assume the outgoing  $\{D, D^*, D_s, D_s^*\}$  and  $D^{**}$  wave functions to have angular momentum  $L=0$  and  $L=1$  respectively. In the lowest radial state the wave functions are:

$$\psi_L(\mathbf{r}) = \mathcal{N}_L r^L Y_{LM_L}(\hat{\mathbf{r}}) \exp(-\beta_L^2 r^2/2) \quad \mathcal{N}_L = \frac{2\beta_L^{3/2}}{\pi^{1/4}} \left\{1, \sqrt{\frac{2}{3}}\beta_L, \frac{2}{\sqrt{15}}\beta_L^2\right\} \quad (6)$$

All wave functions are properly normalized (with the brackets referring to S, P and D states respectively). Performing the differentiation in eqn. 2 gives for  $S + S$  final states

$$\begin{aligned} \mathbf{e}_\sigma^* \cdot (i\nabla_{\mathbf{r}_B} + i\nabla_{\mathbf{r}_C} + \frac{2m}{m+M}\mathbf{p}_B) \psi_S^*(\mathbf{r}_B)\psi_S^*(\mathbf{r}_C) = \\ \mathcal{N}_S^2 \exp(-\beta^2(\frac{\mathbf{r}_A^2}{4} + \mathbf{y}^2)) (-i\beta^2\mathbf{r}_A + \frac{2m}{m+M}\mathbf{p}_B) \end{aligned} \quad (7)$$

and now proceeding to perform the y-integration gives

$$\begin{aligned} \int d^3\mathbf{y} \gamma(\mathbf{r}_A, \mathbf{y}_\perp) \times (\text{eqn. 7}) &= A_{00}^0 \sqrt{\frac{fb}{\pi}} \mathcal{N}_S^2 \bar{\gamma}^0 (-i\beta^2\mathbf{r}_A + \frac{2m}{m+M}\mathbf{p}_B) \exp(-\frac{\beta^2\mathbf{r}_A^2}{4}) \quad (8) \\ \bar{\gamma}^0 &\equiv \int d^3\mathbf{y} \exp(-\beta^2\mathbf{y}^2 - \frac{fb}{2}\mathbf{y}_\perp^2) = \frac{\pi^{3/2}}{\beta(\beta^2 + fb/2)} \end{aligned}$$

Similarly for  $P + S$  final states

$$\begin{aligned} (i\nabla_{\mathbf{r}_B} + i\nabla_{\mathbf{r}_C} + \frac{2m}{m+M}\mathbf{p}_B) \psi_P^*(\mathbf{r}_B)\psi_S^*(\mathbf{r}_C) = \mathcal{N}_S\mathcal{N}_P \exp(-\beta^2(\frac{\mathbf{r}_A^2}{4} + \mathbf{y}^2)) \\ \times [i\sqrt{\frac{3}{4\pi}}\mathbf{e}_{M_L^P}^* + (\frac{r_A}{2}Y_{1M_L}^*(\hat{\mathbf{r}}_A) + yY_{1M_L}^*(\hat{\mathbf{y}})) (-i\beta^2\mathbf{r}_A + \frac{2m}{m+M}\mathbf{p}_B)] \end{aligned} \quad (9)$$

and performing the y-integration, terms linear in  $\mathbf{y}$  (in eqn. 9) vanish

$$\begin{aligned} \int d^3\mathbf{y} \gamma(\mathbf{r}_A, \mathbf{y}_\perp) \times (\text{eqn. 9}) = \\ A_{00}^0 \sqrt{\frac{fb}{\pi}} \mathcal{N}_P\mathcal{N}_S \bar{\gamma}^0 [i\sqrt{\frac{3}{4\pi}}\mathbf{e}_{M_L^P}^* + \frac{r_A}{2}Y_{1M_L}^*(\hat{\mathbf{r}}_A) (-i\beta^2\mathbf{r}_A + \frac{2m}{m+M}\mathbf{p}_B)] \exp(-\frac{\beta^2\mathbf{r}_A^2}{4}) \end{aligned} \quad (10)$$

Since the  ${}^3P_0$ -model [9] corresponds to taking  $f = 0$  in the amplitude above, we see that the flux-tube model amplitude differs from the  ${}^3P_0$ -model amplitude by a factor of  $1 + fb/2\beta^2$  for both  $S + S$  and  $P + S$  final states. This explains the systematics of an earlier calculation [6, table II : compare columns 2 and 3] by Isgur and Kokoski, with  $\beta = 0.4$  throughout. Hence in the approximation where (the final state)  $\beta$  is constant throughout for all mesons, *the flux-tube and  ${}^3P_0$ -models yield identical amplitudes* when normalized to experiment.

The reason why Isgur and Kokoski’s results for the  ${}^3P_0$  and flux-tube models are slightly different, is because they use a cigar-shaped overlap, which modifies the infinite cylinder overlap of eqn. 3 longitudinally away from the  $Q\bar{Q}$ -axis. The small deviation of their results for the two models from one another ( $\sim 5\%$  in width) demonstrates that this overlap, although physically reasonable, makes little quantitative difference on the scale of model errors, and is hence safely neglected, vindicating our choice of flux-tube overlap in eqn. 3.

## B Appendix : Decay amplitudes

### B.1 Lowest radial states

The lowest radial state wave functions were listed in eqn. 6. Defining

$$\tilde{A} = \left( \frac{a\tilde{c}}{9\sqrt{3}} \frac{1}{2} A_{00}^0 \sqrt{\frac{fb}{\pi}} \right) \frac{1}{(1 + fb/(2\beta^2))} 8\pi^{3/4} \frac{\beta_A^{3/2}}{(2\beta_A^2 + \beta^2)^{5/2}} \exp\left(-\left(\frac{M}{m+M}\right)^2 \frac{p_B^2}{2\beta_A^2 + \beta^2}\right) \quad (11)$$

we introduce the partial wave S, P, D and F definitions

$$\begin{aligned} P_1 &= i2\tilde{A} \frac{M}{m+M} p_B (\beta^2 + \frac{m}{M}(2\beta_A^2 + \beta^2)) \\ S_1 &= \sqrt{2}\tilde{A} \frac{\beta}{2\beta_A^2 + \beta^2} (6\beta_A^2(2\beta_A^2 + \beta^2) + 2(\frac{M}{m+M}p_B)^2 (\beta^2 + \frac{m}{M}(2\beta_A^2 + \beta^2))) \\ D_1 &= \sqrt{2}\tilde{A} \frac{\beta}{2\beta_A^2 + \beta^2} 2(\frac{M}{m+M}p_B)^2 (\beta^2 + \frac{m}{M}(2\beta_A^2 + \beta^2)) \\ S_2 &= 2\sqrt{2}\tilde{A} \frac{\beta_A}{2\beta_A^2 + \beta^2} (-3\beta^2(2\beta_A^2 + \beta^2) + 2(\frac{M}{m+M}p_B)^2 (\beta^2 + \frac{m}{M}(2\beta_A^2 + \beta^2))) \\ D_2 &= 2\sqrt{2}\tilde{A} \frac{\beta_A}{2\beta_A^2 + \beta^2} 2(\frac{M}{m+M}p_B)^2 (\beta^2 + \frac{m}{M}(2\beta_A^2 + \beta^2)) \\ P_2 &= -i\frac{8}{\sqrt{15}}\tilde{A} \frac{\beta_A^2}{(2\beta_A^2 + \beta^2)^2} \frac{M}{m+M} p_B (-5\beta^2(2\beta_A^2 + \beta^2) + 2(\frac{M}{m+M}p_B)^2 (\beta^2 + \frac{m}{M}(2\beta_A^2 + \beta^2))) \\ F_2 &= -i\frac{8}{\sqrt{15}}\tilde{A} \frac{\beta_A^2}{(2\beta_A^2 + \beta^2)^2} 2(\frac{M}{m+M}p_B)^3 (\beta^2 + \frac{m}{M}(2\beta_A^2 + \beta^2)) \end{aligned} \quad (12)$$

in terms of which we list the amplitudes in Table 5, consistent with the literature [6].

For  $D^{**}$  final states we employ a  ${}^3P_1/{}^1P_1$  mixing angle  $\tilde{\theta}$  according to the convention [16] :

$$\begin{pmatrix} 1^{+L} \\ 1^{+H} \end{pmatrix} = \begin{pmatrix} \cos \tilde{\theta} & \sin \tilde{\theta} \\ -\sin \tilde{\theta} & \cos \tilde{\theta} \end{pmatrix} \begin{pmatrix} {}^1P_1 \\ {}^3P_1 \end{pmatrix} \quad (13)$$

where  $1^{+L}$  and  $1^{+H}$  indicate the low and high mass states respectively.

### B.2 Radial excitations

Instead of deriving the decay amplitudes for radially excited mesons afresh, it is more immediate to notice that the radially excited wave functions can be related to the lowest radial wave functions by differentiation [32] :

$$\psi_{2S}(\mathbf{r}) = \frac{1}{\sqrt{3!}} \frac{\beta^{3/2}}{\pi^{3/4}} \{3 - 2\beta^2 r^2\} e^{-\frac{1}{2}\beta^2 r^2} = \frac{4}{\sqrt{3!}} \beta^2 \frac{d}{d\beta^2} \psi_S(\mathbf{r})$$

$$\psi_{3S}(\mathbf{r}) = \frac{1}{\sqrt{5!}} \frac{\beta^{3/2}}{\pi^{3/4}} \{15 - 20\beta^2 r^2 + 4\beta^4 r^4\} e^{-\frac{1}{2}\beta^2 r^2} = \frac{2}{\sqrt{5!}} \left\{ 3 + 8\beta^2 \frac{d}{d\beta^2} + 8\beta^4 \frac{d^2}{d^2\beta^2} \right\} \psi_S(\mathbf{r})$$

Table 5: Partial wave amplitudes  $M_L(A \rightarrow BC)$  indicated in terms of the functions defined in eqn. 12 and named in accordance with partial waves  $L = S, P, D$  or  $F$ . Flavour can be incorporated for various final states by multiplying  $M_L(A \rightarrow BC)$  by 1 (for  $D_s D_s, D_s^* D_s^*$ ),  $\sqrt{2}$  (for  $DD, D^* D^*, D_s^* D_s$ ) or 2 (for  $D^* D$ ).

	$M_L(A \rightarrow BC)$		$M_L(A \rightarrow BC)$
${}^3S_1 \rightarrow {}^1S_0 {}^1S_0$	$P_1/\sqrt{2}$	${}^3S_1 \rightarrow {}^3P_2 {}^1S_0$	$-D_1/\sqrt{2}$
${}^3S_1 \rightarrow {}^3S_1 {}^1S_0$	$P_1$	${}^3S_1 \rightarrow {}^3P_1 {}^1S_0$	$S_1/\sqrt{3}$
${}^3S_1 \rightarrow {}^3S_1 {}^3S_1$	$\sqrt{7}P_1/\sqrt{2}$		$D_1/\sqrt{6}$
${}^3P_2 \rightarrow {}^1S_0 {}^1S_0$	$D_2/\sqrt{3}$	${}^3S_1 \rightarrow {}^1P_1 {}^1S_0$	$S_1/\sqrt{6}$
${}^3P_2 \rightarrow {}^3S_1 {}^1S_0$	$D_2/\sqrt{2}$		$-D_1/\sqrt{3}$
${}^3P_1 \rightarrow {}^3S_1 {}^1S_0$	$S_2/\sqrt{3}$		
	$D_2/\sqrt{6}$	${}^3D_1 \rightarrow {}^1S_0 {}^1S_0$	$-P_2$
${}^3P_0 \rightarrow {}^1S_0 {}^1S_0$	$-S_2/\sqrt{6}$	${}^3D_1 \rightarrow {}^3S_1 {}^1S_0$	$P_2/\sqrt{2}$
${}^1P_1 \rightarrow {}^3S_1 {}^1S_0$	$S_2/\sqrt{6}$	${}^3D_1 \rightarrow {}^3S_1 {}^1S_0$	$\sqrt{2}P_2/\sqrt{5}$
	$-D_2/\sqrt{3}$		$3\sqrt{2}F_2/\sqrt{5}$

$$\psi_{2P}(\mathbf{r}) = 4\sqrt{\frac{2!}{5!}} \frac{\beta^{5/2}}{\pi^{1/4}} r \{5 - 2\beta^2 r^2\} Y_{1M_L}(\hat{\mathbf{r}}) e^{-\frac{1}{2}\beta^2 r^2} = 2\sqrt{\frac{2}{5}} \beta^2 \frac{d}{d\beta^2} \psi_{1P}(\mathbf{r})$$

$$\psi_{2D}(\mathbf{r}) = 8\sqrt{\frac{3!}{7!}} \frac{\beta^{7/2}}{\pi^{1/4}} r^2 \{7 - 2\beta^2 r^2\} Y_{2M_L}(\hat{\mathbf{r}}) e^{-\frac{1}{2}\beta^2 r^2} = 2\sqrt{\frac{2}{7}} \beta^2 \frac{d}{d\beta^2} \psi_{1D}(\mathbf{r})$$

$$\begin{aligned} \psi_{4S}(\mathbf{r}) &= -\frac{1}{\sqrt{7!}} \frac{\beta^{3/2}}{\pi^{3/4}} \{105 - 210\beta^2 r^2 + 84\beta^4 r^4 - 8\beta^6 r^6\} e^{-\frac{1}{2}\beta^2 r^2} \\ &= -\frac{8}{\sqrt{7!}} \left\{ 21\beta^2 \frac{d}{d\beta^2} + 24\beta^4 \frac{d^2}{d^2\beta^2} + 8\beta^6 \frac{d^3}{d^3\beta^2} \right\} \psi_S(\mathbf{r}) \end{aligned} \quad (14)$$

The differential operator depends only on  $\beta$ , and can hence be pulled out when the integration in eqn. 2 over  $\mathbf{r}_A$  and  $\mathbf{y}$  is performed. The amplitudes for radially excited meson decay can hence be found by applying the differential operators in eqn. 14 to the amplitudes in table 5.

## References

- [1] M. Mangano, CDF Collaboration, 27<sup>th</sup> *Int. Conf. on High Energy Physics*, Glasgow, 20 - 27 July (1994).
- [2] P. Cho, M.B. Wise, CALT-68-1954, hep-ph/9410214.
- [3] F.E. Close, *Phys. Lett.* **B342** (1995) 369.
- [4] D.P. Roy, K. Sridhar, CERN-TH.7434/94, TIFR/TH/94-33, hep-ph/9409232.

- [5] P. Cho, M.B. Wise, CALT-68-1962, hep-ph/9411303;  
E. Braaten, S. Fleming, NUHEP-TH-94-26, hep-ph/9411365.
- [6] R. Kokoski, N. Isgur, *Phys. Rev.* **D35** (1987) 907.
- [7] N. Isgur, J. Paton, *Phys. Lett.* **124B** (1983) 247; *Phys. Rev.* **D31** (1985).
- [8] P. Geiger, E.S. Swanson, *Phys. Rev.* **D50** (1994) 6855.
- [9] A. Le Yaouanc, L. Oliver, O. Pène, J. Raynal, *Phys. Rev.* **D8** (1973) 2223; **D9** (1974) 1415; **D11** (1975) 1272.
- [10] F.E. Close, P.R. Page, “The dynamics of hybrid charmonium”, R.A.L. and Univ. of Oxford report in preparation (1995).
- [11] E. Eichten *et al.*, *Phys. Rev. Lett.* **34** (1975) 369; **36** (1976) 500; **37** (1976) 477; *Phys. Rev.* **D17** (1978) 3090; **D21** (1980) 203.
- [12] J. Merlin, *D.Phil. thesis*, Univ. of Oxford (1986).
- [13] R. Kokoski, *Ph.D. thesis*, Univ. of Toronto (1984).
- [14] T. Barnes, *private communication*.
- [15] A. Bradley *et al.*, *J. Phys.* **G4** (1978) 1517; *Phys. Lett.* **93B** (1980) 69; *Z. Phys.* **C4** (1980) 67.
- [16] S. Godfrey, N. Isgur, *Phys. Rev.* **D32** (1985) 189.
- [17] A. Le Yaouanc, L. Oliver, O. Pène, J. Raynal, *Phys. Lett.* **71B** (1977) 397; **72B** (1977) 57.
- [18] M. Caichian, R. Kögerler, *Phys. Lett.* **80B** (1978) 105; *Ann. Phys.* **124** (1980) 61.
- [19] V.A. Novikov, L.B. Okun, M.A. Shifman, A.I. Vainshtein, M.B. Voloshin, V.I. Zakharov, *Phys. Rep.* **41** (1978) 1.
- [20] W. Kwong, J.L. Rosner, C. Quigg, *Ann. Rev. Nucl. Part. Sci.* **37** (1987) 325.
- [21] T. Barnes, ORNL-CCIP-93-11, RAL-93-065, hep-ph/9308368.
- [22] J.W. Alcock, M.J. Burfitt, W.N. Cottingham, *Z. Phys.* **C25** (1984) 161.
- [23] N. Isgur, D. Scora, B. Grinstein, M.B. Wise, *Phys. Rev.* **D39** (1989) 799.
- [24] Particle Data Group, *Phys. Rev.* **D50** (1994) 1173.
- [25] F.E. Close, P.R. Page, hep-ph/9411301, RAL-94-116, OUTP-94-29P, *Nucl. Phys.* **Bxxx** (in press); hep-ph/9412301, RAL-94-122, OUTP-94-35P.
- [26] S. Ono, *Phys. Rev.* **D23** (1981) 1118.
- [27] Y.P. Kuang, T.M. Yan, *Phys. Rev.* **D41** (1990) 155.
- [28] Y.B. Ding, D.H. Qin, K.T. Chao, *Phys. Rev.* **D44** (1991) 3562; *Chinese Phys. Lett.* **10** (1993) 460; PUTP-94-08, hep-ph/9502409.



- [29] K. Heikkilä, N.A. Törnqvist, S. Ono, *Phys. Rev.* **D29** (1984) 110.
- [30] F. Guerin, A. Arneodo, J.L. Femenias, *Nucl. Phys.* **B167** (1980) 413.
- [31] S. Perantonis, C. Michael, *Nucl. Phys.* **B347** (1990) 854.
- [32] R. Barbieri, R. Kögerler, Z. Kunszt, *Phys. Lett.* **B56** (1975) 477.
- [33] T. Barnes, F.E. Close, E.S. Swanson, RAL-94-106, hep-ph/9501405; S. Ono, *Z. Phys.* **C26** (1984) 307.
- [34] N. Dowrick, J. Paton, S. Perantonis, *J. Phys.* **G13** (1987) 423.
- [35] F.E. Close, *An Introduction to Quarks and Partons*, Academic Press (1979).
- [36] J.M. Richard, *Z. Phys.* **C4** (1980) 211; G.R. Goldstein *et al.*, *Z. Phys.* **C12** (1982) 23.
- [37] E. van Beveren *et al.*, *Phys. Rev.* **D21** (1980) 772; **D27** (1983) 1527; *Z. Phys.* **C17** (1983) 135; S. Jacobs, K.J. Miller, M.G. Olsson, *Phys. Rev. Lett.* **50** (1983) 1181.

## Figure Captions

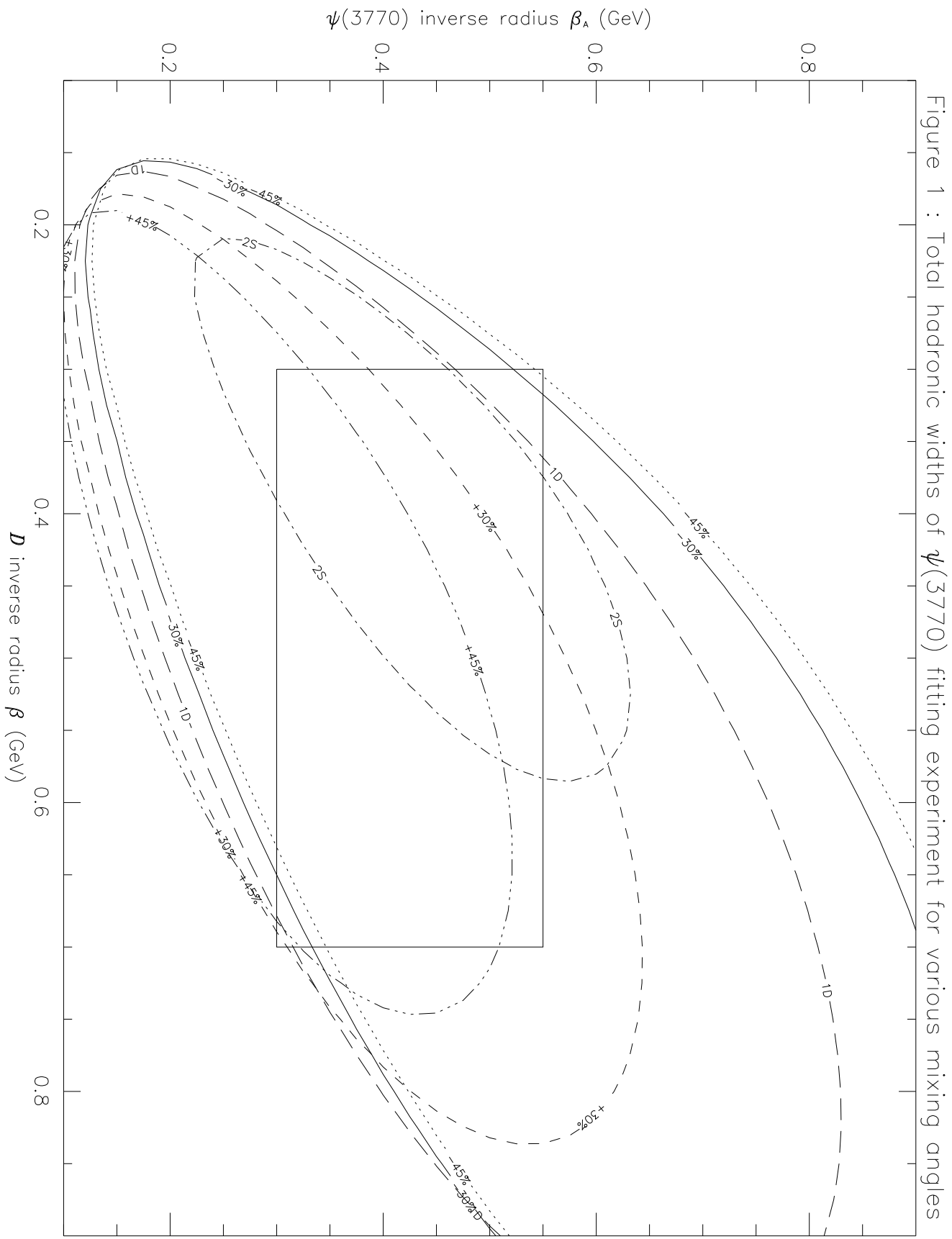
Figure 1: The contours indicate  $\psi(3770)$  total hadronic widths fitting the mean experimental width in eqn. 1. Where there is 1D-2S mixing with mixing angle  $\theta$ , we display  $\sin\theta$  (which can be positive or negative). Pure 1D and 2S states are also shown. The “square” indicates theoretically acceptable parameters.

Figure 2: Total hadronic widths of the higher mass charmonia  $\psi(4040)$ ,  $\psi(4160)$  and  $\psi(4415)$  fitting experiment. For the latter two states the contours enclose narrow regions with experimentally acceptable total widths, as indicated by shading in one case. They indicate  $1\sigma$  variations from the mean experimental width (eqn. 1). We display  $\psi(4160)$  as 3S or 2D, and  $\psi(4415)$  as 4S. The regions in table 4 where  $\psi(4040)$  fits experiment are indicated by three large “dots”. The “square” indicates theoretically acceptable parameters.

Figure 3: Total hadronic widths of the 2P states with  $J^{PC} = 2^{++}$  (3.98 GeV),  $1^{++}$  (3.95 GeV) and  $0^{++}$  (3.92 GeV) [16] for theoretically acceptable parameters. We indicate regions where these states may be narrow. The lighter and darker shading indicate  $2^{++}$  widths less than 5 MeV and 1 MeV respectively. The contours for  $0^{++}$  and  $1^{++}$  enclose narrow regions where widths are less than 5 MeV or 1 MeV.

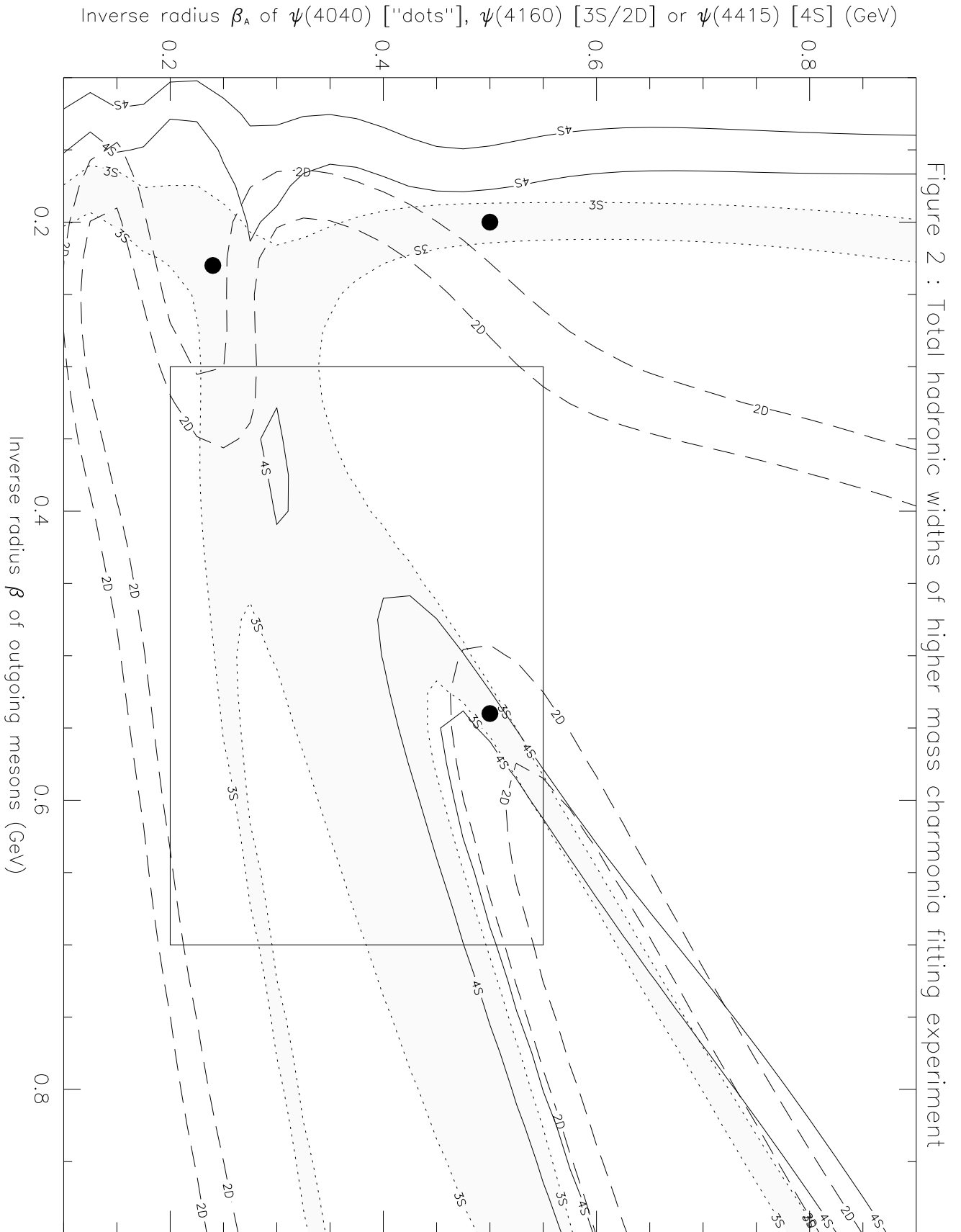
This figure "fig1-1.png" is available in "png" format from:

<http://arxiv.org/ps/hep-ph/9502204v2>



This figure "fig1-2.png" is available in "png" format from:

<http://arxiv.org/ps/hep-ph/9502204v2>



This figure "fig1-3.png" is available in "png" format from:

<http://arxiv.org/ps/hep-ph/9502204v2>

